Ion Extraction Capabilities of Two-Grid Accelerator Systems

Dean C. Rovang* and Paul J. Wilbur†
Colorado State University, Fort Collins, Colorado

An experimental investigation into the ion extraction capabilities of two-grid accelerator systems common to electrostatic ion thrusters is described. A large body of experimental data that facilitates the selection of the accelerator system geometries and operating parameters necessary to maximize the extracted ion current is presented. Results suggest that the impingement-limited perveance is not dramatically affected by reductions in the screen hole diameter to 0.5 mm. Impingement-limited performance is shown to depend most strongly on the grid separation distance, accelerator hole diameter ratio, discharge-to-total accelerating voltage ratio, and net-to-total accelerating voltage ratio. Results obtained at small grid separation ratios suggest a new grid operating condition where high levels of beam current per hole are achieved at a specified net accelerating voltage. It is shown that this operating condition is realized at an optimum ratio of net-to-total accelerating voltage ratio which is typically quite high. The apparatus developed for this study is also shown to be well suited for measuring the electron backstreaming characteristics of two-grid accelerator systems. Backstreaming data are presented for a wide range of geometries and operating conditions.

Introduction

TO reduce the number of electrostatic ion thrusters required for a space propulsion mission and hence the cost and mass of the thruster subsystem, it is generally desirable to increase the thrust densities of these devices above those attainable with currently available ion thrusters. To keep the thrusters operating at their optimum specific impulse, this should be accomplished by increasing the ion beam current density extracted through the ion optics system without increasing the exiting ion velocity. However, previous research[1-10] has generally focused on the ion beam divergence characteristics of the accelerator systems rather than the phenomena that limit the extractable ion current density. The present investigation was undertaken to provide a more complete understanding of the phenomena that limit the ion extraction capabilities of two-grid accelerator systems. This investigation deals with the effects of variations in the accelerator system geometry and operating conditions of the ion thruster on these ion extraction-limiting phenomena. A rather complete picture of the ion extraction capabilities of two-grid accelerator systems is provided because of the extended range of geometries and operating conditions over which these limiting phenomena are investigated.

The geometrical and potential difference definitions used in this study are defined in Fig. 1 where a single ion beamlet/grid system cross section and typical axial potential profiles are shown. Grid performance data will be presented in terms of normalized perveance per hole defined by the equation

$$P=\frac{J}{V_T^{3/2}}\left(\frac{\ell_e}{d_s}\right)^2 \tag{1}$$

where J is the beam current per hole and the other quantities are defined in Fig. 1. Equation (1) is based on a one-dimensional analysis of the ion extraction process. Since both the beamlet suggested in Fig. 1a and the actual beamlets are not one-dimensional, some alteration of the one-dimensional solution is required. Traditionally, this has been accomplished by using an effective acceleration length[5,8] in place of the grid separation distance ℓ_g. This length (shown in Fig. 1a) is defined by

$$\ell_e=\left[\ell_g^2+(d_s^2/4)\right]^{1/2} \tag{2}$$

All of the tests were conducted on an ion source 8 cm in diameter and 10 cm long with a mildly divergent magnetic field. The magnetic field was derived from a long solenoidal winding wrapped around the outside of the thruster body. Except for a cylindrical copper anode, nonmagnetic stainless steel construction was employed throughout the source. Tungsten filaments heated by an alternating current were used for both the neutralizer and discharge cathodes. This source was designed to be stable and to provide the high current density capability needed to assure a proper test of the grids.

The grids were made from thin sheets of graphite. The grid aperture pattern used a 19 hole hexagonal array with a center-to-center hole spacing of 2.5 mm. This fixed hole spacing resulted in a considerable reduction in the open area fraction for the smaller screen hole diameters. While the experiments were not designed specifically to study the effects of grid open area fraction on ion extraction performance, no unusual behavior that could be attributed to changes in the fraction were observed. The extraction region of the grids was masked down to a small area (~ 1 cm^2) near the axis of the source to help insure ion extraction from a uniform plasma over the hole pattern. The geometries of the grids were varied by selecting different diameter drills with which to machine the hole patterns in the various thicknesses of the graphite sheets.

Because the grid separation distance is a very important parameter, the test apparatus has been designed so that the grid separation can be varied while the ion source is being operated. This is accomplished, using the apparatus shown schematically in Fig. 2, by moving the fork-shaped wedge in the manner suggested by the large arrow. As this wedge is moved toward the grids, it forces the accelerator and screen grid support plates apart, thus separating the screen and ac-

Received July 30, 1984; revision received Feb. 18, 1985.

*Research Assistant (presently, Technical Staff Member, Sandia Laboratories, Albuquerque, N. Mex.). Member AIAA.

†Professor, Department of Mechanical Engineering. Member AIAA.

celerator grids attached to these plates. All of the materials used in the construction of this apparatus are capable of withstanding high temperatures. Graphite was used for both the grids and grid support plates to minimize the differential thermal expansion between these components that could cause grid warpage. The distance between the points at which the grids were attached to the support plates was also shortened to minimize the effects of grid warpage and deflection due to the attractive electrostatic forces between the grids. Alignment of the grids, which is accomplished by positioning and clamping each grid and then checking the alignment with a large illuminated magnifying glass, is maintained during operation by the boron nitride guideposts shown in Fig. 2. Electrical isolation is assured by the sheet of isomica between the screen grid support plate and the wedge. The wedge is mechanically connected to a micrometer used to measure and adjust its translation from outside the vacuum system.

Immediately after each period of data collection, while the source was still hot, the grid separation distance was reduced until the measured electrical resistance between the grids became essentially zero. This reference point on the micrometer (assumed to correspond to zero separation) along with the geometry of the wedge could then be used to calculate the grid spacing from the micrometer readings recorded during a test. Because this procedure for defining the reference point was conducted while the grids were hot, errors in the grid separation caused by thermal warpage were minimized.

The ion extraction performance of each grid was investigated over an essentially continuous range of net-to-total accelerating voltages and grid separations and at the values of the geometrical and operating parameters given in Table 1.

After allowing the source to warm up, data collection was begun with the accelerator system operating at a large grid separation and a high ratio of net-to-total accelerating voltage, typically $R=0.8$. The propellant flow rate was adjusted to the minimum at which the source operated stably over the full range of beam currents investigated. The conduct of the tests involved increasing the cathode emission current in steps and measuring the beam and impingement currents at each step until the impingement current reached a high value ($\gtrsim 10\%$ of the beam current). The cathode emission current was then reduced, the ratio of net-to-total accelerating voltage lowered to the next value of interest, and the data collection procedure repeated at the same propellant flow rate. After the range of net-to-total accelerating voltage ratios of interest had been investigated, the grid separation was reduced slightly and the entire procedure repeated. The test was stopped when the grids were so closely spaced that electrical breakdown between them seemed likely. For all of the testing described here, the magnet current was set to induce a magnetic field strength of approximately 35 G at the screen grid and 45 G near the upstream end of the discharge chamber. The bell jar pressure was primarily a function of the propellant flow rate and varied within the range of $1.0\text{-}5.0\times10^{-5}$ Torr for the tests. Unless stated otherwise, the discharge voltage was maintained at 45 V.

The collection of backstreaming data for each grid geometry was accomplished by reducing the magnitude of the accelerator grid potential while watching for the rather sudden increase in beam current that is indicative of electrons backstreaming into the discharge chamber. Care was taken to identify as closely as possible the exact accelerator grid potential at which the slightest increase in beam current was observed. Beam current increases of 1% were generally sufficient to insure that backstreaming was occurring. The accelerator grid voltage at the onset of backstreaming are considered accurate to within a few volts.

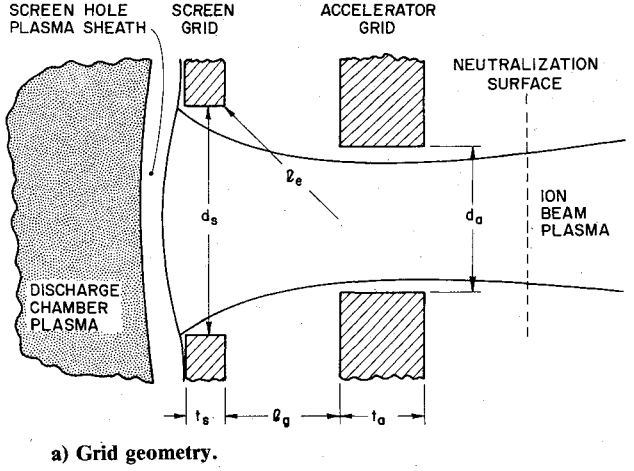

a) Grid geometry.

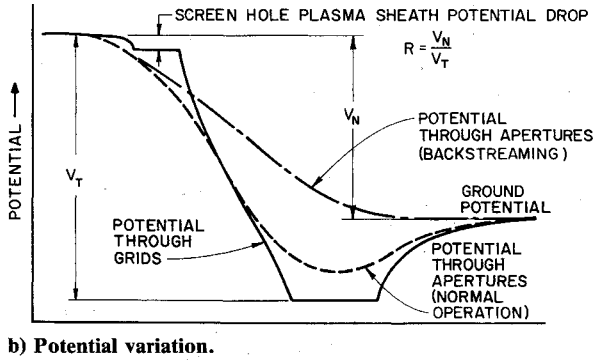

b) Potential variation.

Fig. 1 Two-grid acceleration system.

Table 1 Grid parameter values investigated

Screen hole diameter d_s	0.5, 1.0, 1.5, 2.0[a] mm
Accelerator hole diameter ratio d_a/d_s	0.66, 0.81,[a] 1.0
Screen grid thickness ratio t_s/d_s	0.13, 0.25,[a] 0.38
Accelerator grid thickness ratio t_a/d_s	0.13, 0.25,[a] 0.38, 0.51
Discharge-to-total voltage ratio V_D/V_T	0.05, 0.10,[a] 0.15

[a]Designates value for standard configuration.

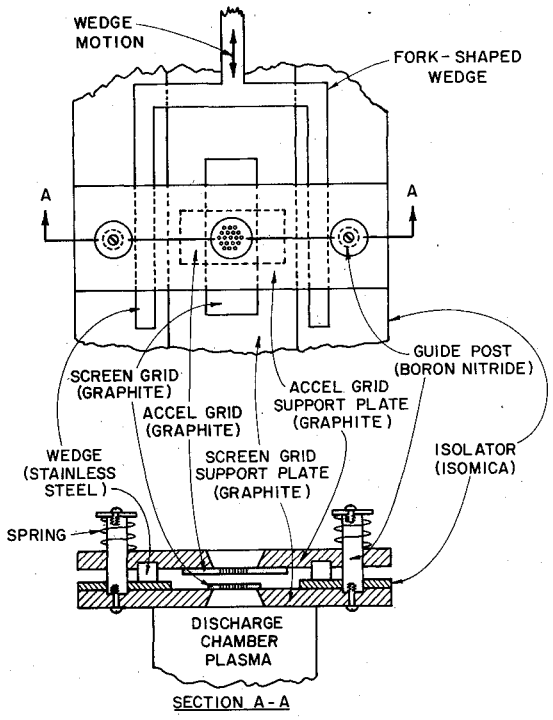

Fig. 2 Variable grid spacing apparatus.

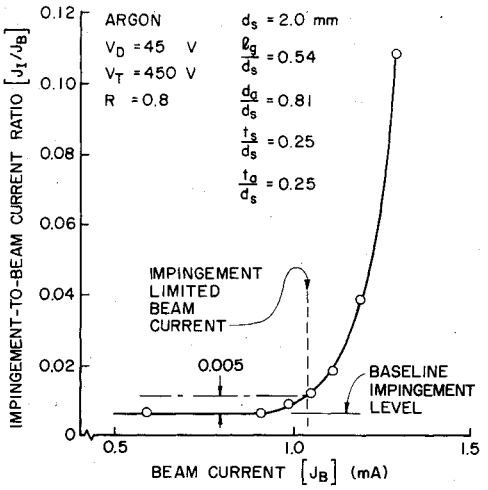

Fig. 3 Typical impingement curve.

Ion Extraction Test Results

Definition of Impingement-Limited Operation

Figure 3 displays a typical curve showing how the impingement current (normalized by the corresponding beam current) varied as a function of beam current. At low beam currents, the curve is horizontal and the impingement-to-beam current ratio is constant at a baseline impingement level determined by the rate at which charge exchange ions strike the accelerator grid. As the beam current is increased, the curve in Fig. 3 begins to depart from the baseline level and the impingement current rises abruptly. This increase in impingement current above the baseline level is due to the direct impingement of high-velocity ions on the accelerator grid. Instead of presenting all of the performance data in the form shown in Fig. 3, it is more convenient and more meaningful for comparison purposes to define an impingement-limited beam current, i.e., the beam current at which the direct accelerator grid impingement current becomes excessive. For this paper, the impingement-limited condition is said to occur when the onset of direct ion impingement results in an increment of 0.005 in the ratio of the impingement-to-beam current above the baseline impingement level. The magnitude of this incremental increase, although somewhat arbitrary, was selected as a compromise between two competing considerations. It is large enough to insure that the increase in the impingement current was indeed due to direct ion impingement and not a result of impingement current noise. On the other hand, it is small enough to insure that the direct ion impingement is sufficiently low so as not to pose a problem for an operating grid set. The beam current associated with this impingement-limited condition is denoted by the dashed line in Fig. 3.

For a given test, the total accelerating voltage, grid separation distance, and hole size are known. Therefore, the impingement-limited beam current can be divided by the number of apertures to obtain the current per hole. The impingement-limited normalized perveance per hole is calculated from this information using Eq. (1). The normalized perveance based on this definition will be used to make comparisons of the ion extraction capabilities of the various grid geometries investigated over a large range of operating conditions.

Effect of Net-to-Total Accelerating Voltage Ratio

When results such as those of Fig. 3 are obtained over a range of separation distances and then impingement-limited normalized perveances are computed in the manner just described, one obtains curves like those shown in Fig. 4. In this figure, the impingement-limited normalized perveance per hole is plotted as a function of the grid separation normalized

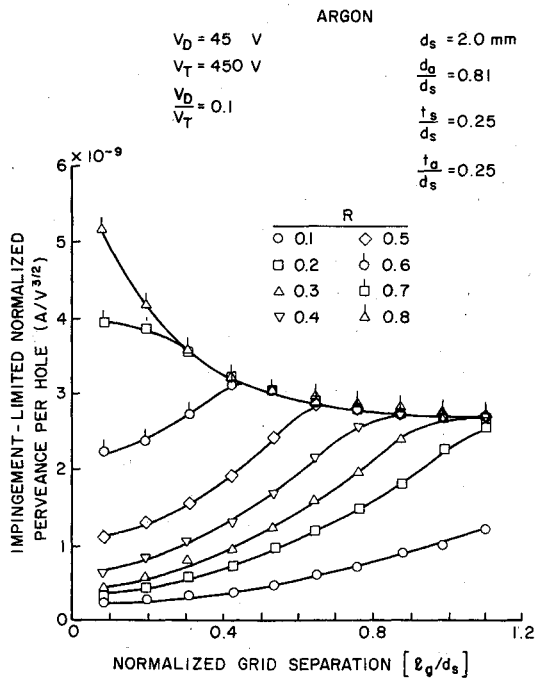

Fig. 4 Effect of net-to-total accelerating voltage ratio on ion extraction performance.

to the screen hole diameter for various ratios of the net-to-total accelerating voltage ratio. It is observed that increases in the ratio of net-to-total accelerating voltage always result in increased perveance (improved extraction performance) at close grid separations. However, it is seen that all of the curves tend to converge to a single perveance at larger grid separations. If the impingement-limited normalized perveance per hole were a perfect normalizing parameter over the complete range of grid separations and net-to-total accelerating voltage ratios, all of the curves would be coincident horizontal lines. Figure 4 shows that this condition tends to occur only at large grid separations. It is therefore argued that departures from this single value at close grid separations represent departures from the one-dimensional model on which the normalized perveance per hole is based. The reduction in perveance at low values of R has also been observed by Aston et al.[8] Although Aston et al. reported large variations in beam divergence with R, his data did not indicate as dramatic an effect of R on the impingement-limited perveance per hole as that suggested by the results of Fig. 4. The main reason for this is considered to be due to the fact that Aston's investigation was conducted primarily at the larger grid separation ratios where single values of perveance are obtained.

The curves in Fig. 4 characterize the ion extraction performance of the accelerator system geometry defined by the parameters d_a/d_s, t_s/d_s, t_a/d_s, d_s, and the ratio of discharge-to-total voltage V_D/V_T noted at the top of Fig. 4. The effect of variations in these parameters on the ion extraction performance will be considered below. Instead of trying to compare the ion extraction performance using all of the ratios of net-to-total accelerating voltage shown in Fig. 4, representative high ($R=0.8$), medium ($R=0.5$), and low ($R=0.2$) ratios have been selected to indicate the general trends.

Effect of Discharge-to-Total Voltage Ratio

The effect of the ratio of discharge-to-total voltage on ion extraction performance is shown in Fig. 5. At large ratios of net-to-total accelerating voltage ($R=0.8$), it is seen that lower ratios of discharge-to-total voltage result in increased perveances over the entire range of the grid separations investigated. Similar trends hold true for the lower values of R, but it is observed that at close grid separations the curves con-

verge onto a single curve. In general, lower ratios of discharge-to-total voltage result in improved ion extraction performance. This trend has been reported previously by Aston et al.[8] and explored in more detail by Kaufman.[11] Kaufman theorized that the relative effects of the discharge and total accelerating voltage on the plasma sheath cause the sheath to flatten out at high ratios of discharge-to-total voltage and thus result in the onset of impingement at lower perveances. Sheath profile data obtained by Aston and Wilbur[12] confirm this relative effect of discharge voltage on the contour of the sheath upstream of the screen hole.

Additional tests[13] showed the ion extraction performance data obtained at a particular ratio of discharge-to-total voltage was independent of the total accelerating voltage. Consequently, the ion extraction performance data obtained at one total voltage may be assumed to apply for any total voltage as long as the ratio of discharge-to-total voltage remains the same. Recently, this invariance of the impingement-limited perveance with total voltage for a fixed geometry and discharge-to-total voltage ratio was verified in an independent investigation.[14]

Effect of Accelerator Aperture Diameter

Figure 6 shows the effect of variations of the accelerator hole diameter ratio d_a/d_s on impingement-limited perveance. In general, it is observed that larger accelerator holes facilitate operation at higher perveances and therefore higher beam currents. The largest differences are seen over the entire range of grid separations for a net-to-total accelerating voltage ratio equal to 0.8. At this same net-to-total accelerating ratio, it is observed that the curve for the largest accelerator hole diameter ratio ($d_a/d_s = 1.0$) does not extend to very low grid separations. In this case, it is not possible to operate at grid separation ratios below ~ 0.4 because of the occurrence of electron backstreaming. It should be noted that some of the other geometries were near the electron backstreaming limit at very close grid separations when operating at a net-to-total accelerating voltage ratio of 0.8. However, it is emphasized that caution was exercised not to include any data in the ion extraction performance results that might have been influenced by electron backstreaming.

The data of Fig. 6 also show that for $R = 0.8$ the perveance for the smallest accelerator hole diameter ratio (0.66) remained relatively constant as a function of grid separation instead of increasing to larger perveances at close grid separations, as was the case for the medium ratio ($d_a/d_s = 0.81$). It is noteworthy that a similar trend to larger perveances at close grid separations was observed for the smallest accelerator hole diameter ratio ($d_a/d_s = 0.66$), but only at ratios of discharge-to-total voltage below the 0.1 value appropriate to the data of Fig. 6.

The trend of decreased ion extraction performance with decreased accelerator hole diameter was expected and has been reported in previous experimental and theoretical investigations.[5,8] There is, however, an exception that is of particular interest. At close grid separations for $R = 0.5$, it is seen that the impingement-limited perveance for the largest accelerator hole diameter ratio tested ($d_a/d_s = 1.0$) falls slightly below that for the medium ratio ($d_a/d_s = 0.81$). This is believed to be a real effect and will be discussed in greater detail later in this paper.

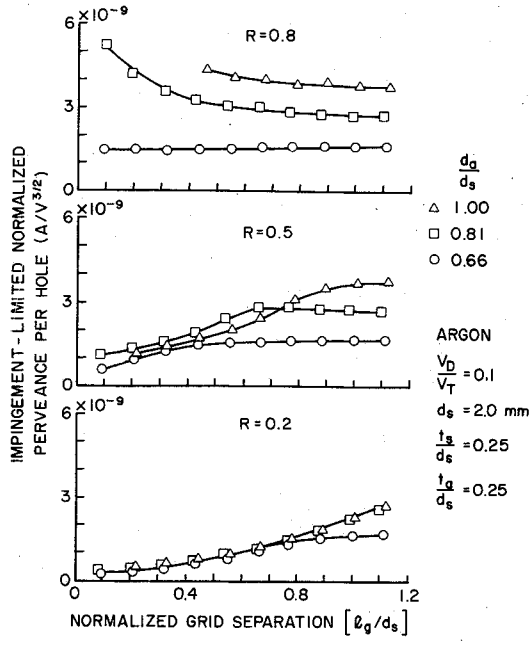

Fig. 6 Effect of accelerator hole diameter.

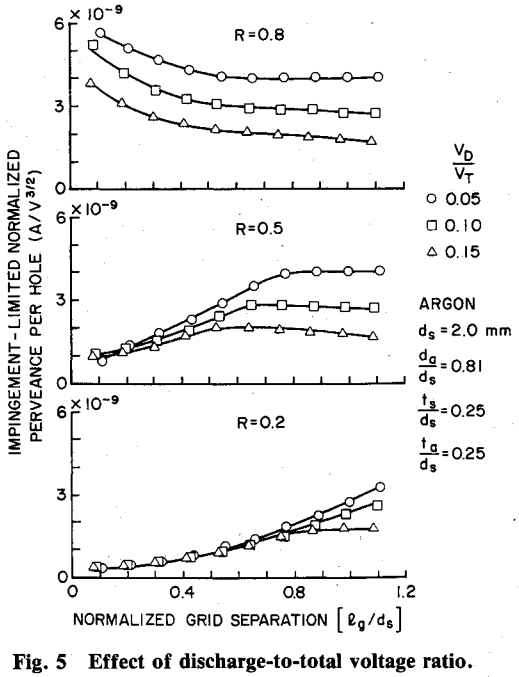

Fig. 5 Effect of discharge-to-total voltage ratio.

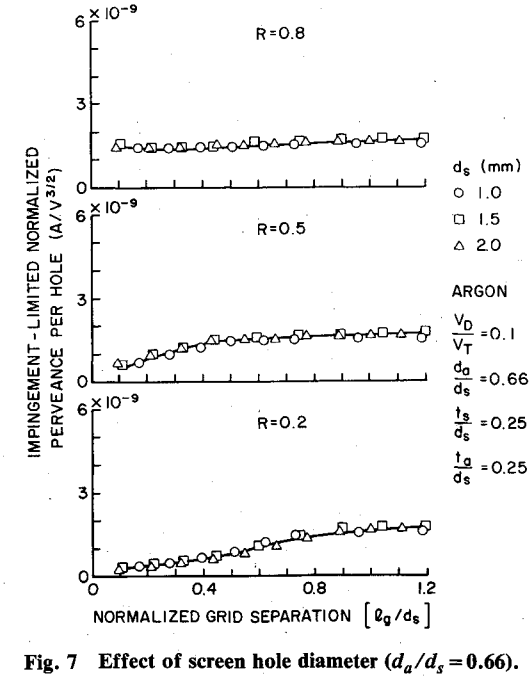

Fig. 7 Effect of screen hole diameter ($d_a/d_s = 0.66$).

Effects of Grid Thickness

The effects of variations in screen grid thickness were also investigated.[13] In general, the results showed that variations in grid thickness do not have a significant effect on ion extraction performance. A consistent trend toward decreased perveance levels with increased screen grid thicknesses was observed. For both the screen and accelerator grid, the most noticeable effect of thickness was observed at close grid separations operating at high ratios of net-to-total accelerating voltage. Even in this operating regime, however, the results show that there is relatively little effect with changes in grid thicknesses for $t_s/d_s \lesssim 0.25$ and $t_a/d_s \lesssim 0.38$.

Effect of Screen Grid Hole Size

A major consideration of this study was the investigation of the effect of operating with screen grid hole diameters below 2.0 mm on ion extraction performance. In Figs. 7-9 the impingement-limited perveance levels obtained with screen grid hole diameters smaller than 2.0 mm are compared to those obtained with 2.0 mm diameter holes. Figures 7 and 8 compare the performance of 1.0, 1.5, and 2.0 mm diameter holes for accelerator hole diameter ratios of 0.66 and 1.00, respectively. These figures do not appear to show any consistent trends that would indicate a decrease in performance with decreasing hole size. This observed independence of ion extraction performance with hole size for diameters as small as 1 mm confirm the preliminary results from this study that were reported in a previous paper.[15] Similarly, this observation has been verified recently in an independent investigation for screen grid hole diameters as small as 1.0 mm.[16] It should be noted that the grids with 1.0 and 1.5 mm diameter screen grid holes were manufactured and aligned in a similar fashion to those with 2.0 mm diameter holes. Using this conventional method of construction and alignment, attempts were made to extend the operation to screen grid hole diameters of 0.5 mm. These results suggested a decrease in ion extraction performance below the levels obtained for the large-diameter holes. The inability to align these smaller holes was suspected to be the cause of the poor performance. In order to insure alignment, in a separate test the accelerator grids were ion machined in situ.[17] This machining process yielded a slight spread (± 0.05 mm) in accelerator hole diameters with an average diameter of 0.4 mm. In Fig. 9, the perveance levels obtained in this test are compared to those of the 2.0 mm diameter holes for an accelerator hole diameter ratio of 0.81 and a discharge-to-voltage ratio of 0.15. The similarity of perveance levels shown in Fig. 9 suggest that accelerator system operation without reductions in ion extraction performance is possible with screen grid hole diameters as small as 0.5 mm. This observation differs from what was expected based on previous experimental investigations[8,18-20] that reported a decrease for screen grid hole diameters below 2.0 mm.[8] The reason for this disparity remains uncertain. However, based on the results and observations made during this investigation, certain possible explanations can be theorized.

It was noted above that only after hole alignment was insured for the 0.5 mm diameter screen grid holes did the performance return to the levels obtained with the larger diameter

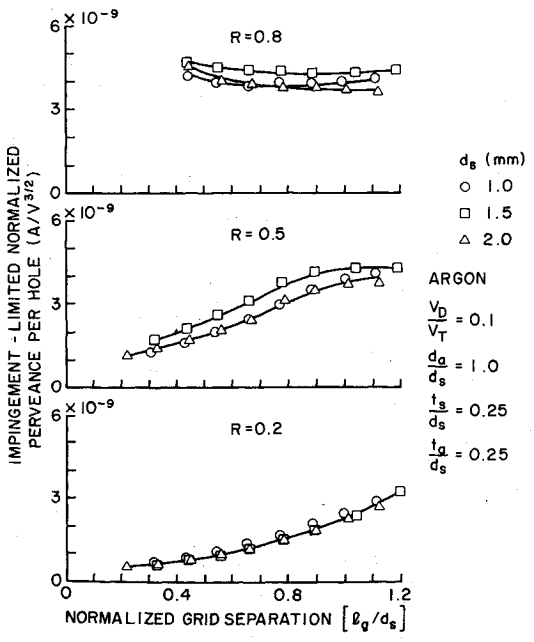

Fig. 8 Effect of screen hole diameter ($d_a/d_s = 1.0$).

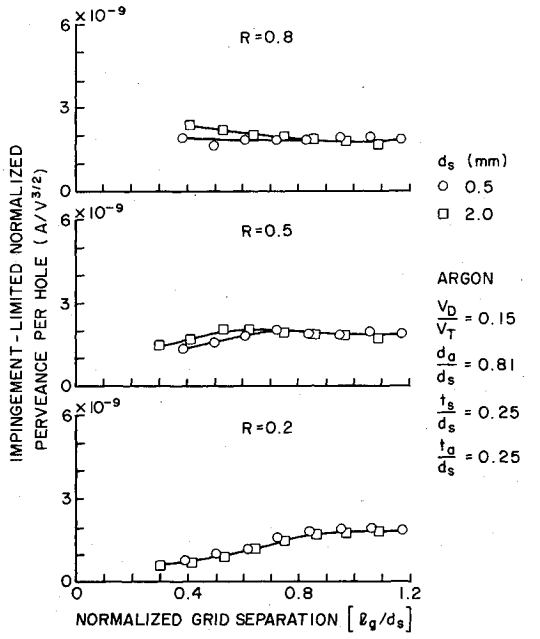

Fig. 9 Effect of screen hole diameter ($d_s = 0.5$ mm).

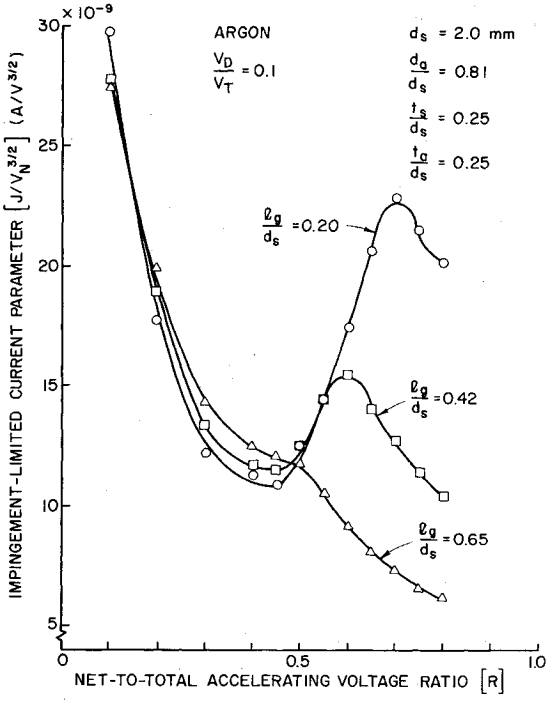

Fig. 10 Effect of grid separation on impingement-limited current parameter.

holes. Based on this observation, it is proposed that misalignment of the screen and accelerator holes represents a likely explanation for the reductions in performance observed previously. It is also noteworthy that the conventional hole alignment technique used in this study differed somewhat from that of the previous investigations reporting reductions of 2.0 mm. The variable grid spacing apparatus used in this study allowed the holes to be aligned with the grids touching; they were separated for testing later. In the previous investigations, the grid systems required alignment of the holes with the grids separated. Another consideration is that other investigations, except for one by Aston et al.,[8] were conducted with large-diameter accelerator systems with thousands of holes. Their complexity makes the alignment of smaller holes more difficult. In any case, it should be emphasized that hole alignment is considered crucial to the success of operating with small screen hole diameters.

Tests also showed the stability of the discharge chamber plasma influenced ion extraction performance. During a segment of the tests, the discharge chamber was changed to a design that operated less stably (arc discharge noise was apparent on an oscilloscope). The onset of high impingement currents occurred at lower perveance levels with this design than it did with the more stable one. This suggests that previous attempts to operate with smaller holes and higher current densities may have resulted in decreased performance due to unstable discharge chamber operating conditions. Other parameters related to the discharge chamber that were determined to influence the ion extraction performance were the condition of the anode surface and the propellant flow rate. Their respective effects on the ion extraction performance results are discussed in more detail in Ref. 13.

Application to Design

Although the impingement-limited normalized perveance per hole is useful for correlating data, it is not easy to use directly to describe at what grid separation ratio and ratio of net-to-total accelerating voltage one should operate in order to maximize the beam current or beam current density for a specified net accelerating voltage. This information can, however, be obtained from curves similar to those shown in Fig. 4, if one assumes that, for a particular ratio of discharge-to-total voltage, these same curves would be obtained at other total accelerating voltage levels. Fortunately, this independence of the impingement-limited normalized perveance curves from the total accelerating voltage has been demonstrated.[13] Thus, for source operation at the minimum flow rate required for stable operation, the impingement-limited normalized perveance per hole P_I is primarily a function of the net-to-total accelerating voltage ratio, the ratio of the discharge-to-total voltage, and the grid geometry, i.e.,

$$P_I = P_I\left(R, \frac{D_D}{V_T}, \frac{\ell_g}{d_s}, \frac{d_a}{d_s}, \frac{t_a}{d_s}, \frac{t_s}{d_s}\right) = \frac{J}{V_T^{3/2}}\left(\frac{\ell_e}{d_s}\right)^2 \quad (3)$$

Dividing Eq. (3) by $R^{3/2}$ and $(\ell_e/d_s)^2$ yields

$$\frac{J}{V_N^{3/2}} = P_I\left(R, \frac{V_D}{V_T}, \frac{\ell_g}{d_s}, \frac{d_a}{d_s}, \frac{t_s}{d_s}, \frac{t_a}{d_s}\right) R^{-3/2}\left(\frac{\ell_e}{d_s}\right)^{-2} \quad (4)$$

The term on the left, which will be referred to as the impingement-limited current parameter, is useful because it facilitates a comparison of the maximum current per hole as a function of the net accelerating voltage rather than the total accelerating voltage. Typical results showing impingement-limited current parameter as a function of R are shown in Fig. 10 for three different grid separation ratios. These particular results are based on data taken from Fig. 4 plus additional data collected at net-to-total accelerating voltage ratios of 0.45, 0.55, 0.65, and 0.75. Figure 10 shows that the highest beam currents per hole are achieved at the lowest net-to-total accelerating voltage ratios and that the magnitudes of these currents are relatively independent of the grid separation. At small grid separation ratios, high current levels are also achieved at an optimum ratio of net-to-total accelerating voltage. The peaks in the curves of Fig. 10 at these optimum R values represent the maximum currents achievable at close grid separations and high ratios of net-to-total accelerating voltage. It should be noted that even higher beam currents could presumably be realized at the peak by further reducing the grid separation and operating at R values above ~ 0.70 where the $\ell_g/d_s = 0.2$ curve peaks. The grid separation could presumably continue to be reduced until the onset of electron backstreaming or electrical breakdown occurred.

For operation at high beam current density levels, the results of Fig. 10 seem to suggest the choice of operating at low ratios of net-to-total accelerating voltage or at high ratios of net-to-total accelerating voltage and small grid separation ratios. However, because of some other considerations, this observation is not as straightforward as it may first appear. To illustrate, a design example using the results of Fig. 10 is considered.

The results of Fig. 10 suggest that similar values of the impingement-limited current parameter ($\sim 22.5 \times 10^{-9}$ $A/V^{3/2}$) would be obtained by operating either at the peak of the curve for $\ell_g/d_s = 0.2$ where $R \cong 0.7$ or at a net-to-total accelerating voltage ratio of 0.15. The interesting thing to note about operating at $R = 0.15$ is that for the range of normalized grid separation appropriate to Fig. 10 ($0.2 < \ell_g/d_s < 0.65$) the impingement-limited current parameter appears to be independent of the grid separation ratio. Because of manufacturing and mechanical design constraints, one of the first dimensions usually specified in the design of a large-diameter accelerator system is the grid separation distance necessary to maintain a minimum span-to-gap ratio. Under the constraint of maintaining this design-limited grid separation distance, operation at larger grid separation ratios could be accomplished by selecting smaller screen grid holes. These smaller screen grid holes would facilitate more holes per unit area of the grids and thus higher beam current densities. In the particular case under consideration here, for a fixed grid separation distance, an increase in the grid separation ratio from 0.2 to 0.65 translates roughly into a screen hole diameter three times as small. Since the area of the hole scales with the square of hole diameter, this means that approximately nine times as many holes could fit into the same size accelerator system and, as a result, a ninefold increase in current density could be achieved. From the standpoint of obtaining higher densities, the preceding comparison suggests that, when the grid separation distance is fixed, it is advantageous to operate with smaller holes at low ratios of net-to-total accelerating voltage and large grid separation ratios as opposed to high ratios of net-to-total accelerating voltage and small grid separation ratios.

Besides current density, there are other considerations that need to be addressed when trying to decide between operation at high or low values of R. Some disadvantages of operation at low net-to-total accelerating voltage ratios with two grids are: 1) higher total voltages that increase the likelihood of electrical breakdown, 2) more divergent ion beams, 3) a greater sensitivity of impingement current to changes in beam current,[13] 4) higher baseline impingement current levels,[13] and 5) more energetic charge exchange ions that shorten the accelerator grid lifetime.

All of these disadvantages must be weighed against the advantage of obtaining higher beam current densities by operating with low ratios of net-to-total accelerating voltage and large grid separation ratios as compared to operating at high ratios of net-to-total accelerating voltage and small grid separation ratios. The only perceived disadvantage of operating at high ratios of net-to-total accelerating voltage is the greater likelihood of electron backstreaming. A detailed

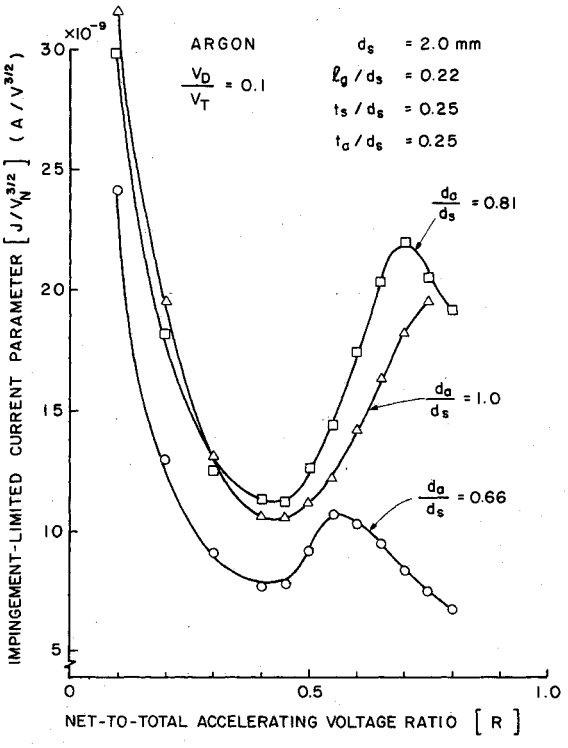

Fig. 11 Effect of accelerator hole diameter on impingement-limited current parameter.

example of how to use ion extraction performance data to design a grid system is presented in Ref. 13.

The usefulness of the impingement-limited current parameter as a design tool is further demonstrated in Fig. 11. In this figure the impingement-limited current parameter is plotted as a function of the ratio of net-to-total accelerating voltage for three different accelerator hole diameter ratios operating at the same normalized grid separation. The most interesting point to be made concerning the results shown in Fig. 11 is that, at larger ratios of net-to-total accelerating voltage, the highest impingement-limited current levels are obtained not with the largest accelerator hole diameter but rather with the second largest. This is an important result because it is preferable from the discharge chamber viewpoint to operate with smaller accelerator grid holes in order to minimize the loss of unionized propellant. Heretofore, it has generally been accepted that grids should be operated with the largest possible accelerator grid holes ($d_a/d_s = 1.0$) to achieve the highest beam currents. Hence, the objectives for high beam currents and low neutral propellant loss are in conflict. However, the results of Fig. 11 suggest that at small grid separations ratios and medium-to-high ratios of R, it is sometimes unnecessary and even self-defeating to try to achieve higher beam currents by utilizing very large accelerator hole diameter ratios ($d_a/d_s = 1.0$). It should be noted that the data point for $d_a/d_s = 1.0$ and $R = 0.8$ was not included in Fig. 11 because of the occurrence of electron backstreaming.

Electron Backstreaming Results

Because the variable grid spacing apparatus facilitated operation over a wide range of grid separations, this apparatus was found to be well suited for measuring the electron backstreaming characteristics of the various grid pairs used in this investigation. All of the experimental electron backstreaming data obtained with the different grid geometries for a screen grid hole diameter of 2.0 mm are correlated in Fig. 12. These data were obtained at beam currents near the impingement limit. In Fig. 12, the backstreaming limit R_{max} is plotted as a function of the effective normalized length $\ell_e/d_a \cdot \exp(t_a/d_a)$. This effective length developed by a previous researcher[21] is

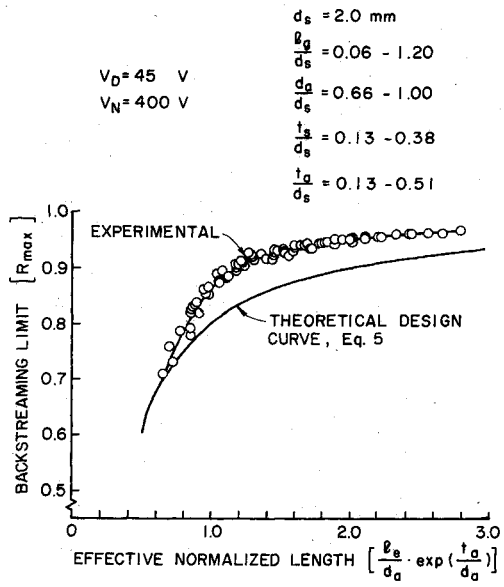

Fig. 12 Backstreaming correlation.

seen to correlate the data from a wide range of geometries quite well. Also shown in Fig. 12 is the theoretical design curve proposed by Kaufman[5] and given by the equation

$$R_{max} = 1 - \frac{0.2}{\ell_e/d_a \cdot \exp(t_a/d_a)} \tag{5}$$

Qualitatively, the experimental and theoretical curves have the same shape. At values of the effective normalized length above ~0.8, the theoretical curve is seen to be more conservative. Because the data were collected over a wide range of operating conditions and because the geometric effects seem to be reflected properly in the effective length parameter, Fig. 12 can be used as a design curve. Accelerator system operation without electron backstreaming could be expected by operating in the area below and to the right of the experimental curve; operation above it would result in electron backstreaming. The effect of the ion beam current or perveance on the electron backstreaming limit was investigated.[13] It was found that operation at slightly higher ratios of net-to-total accelerating voltage than those indicated in Fig. 12 before electron backstreaming occurred. The data of Fig. 12 were collected at 400 V net accelerating voltage and it is noted that other data[13] showed that increases in this voltage to 600 V did not change the results. Decreases in net accelerating voltage to 200 V caused a slight increase in the backstreaming limits shown in Fig. 12 at low normalized grid separations. The screen grid hole size, while having a minor effect on the backstreaming results, did tend to allow operation at slightly higher ratios of net-to-total accelerating voltage before electron backstreaming occurred. It was also observed that the magnitude of increases in the electron backstreaming limit became significant (above the spread of data shown in Fig. 12) only for screen hole diameters below 1.5 mm. While the reason is uncertain, it is possible this trend toward higher backstreaming limits with decreasing hole size might be related to an increase in the grid webbing area between the hole that accompanied reductions in the screen hole diameters in the present experiments. This occurred because the hole-to-hole spacing was held fixed while the diameter was varied. It is also possible that this effect of hole size on backstreaming might somehow be related to the plasma sheath thickness downstream of the accelerator grid. It is speculated that the distance between the accelerator grid and neutralization surface did not

scale in proportion to the dimensions of the smaller grid geometries.

Conclusions

The basic relationships defining the current extraction capabilities of ion optic systems appear to be valid for screen grid hole diameters as small as 0.5 mm. It is expected that these relationships would be valid for even smaller holes, provided the ion source discharge operated stably and the accelerator system were sufficiently sound so that proper hole alignment and grid separation could be maintained. The ion extraction performance of two-grid accelerator systems is a strong function of the net-to-total accelerating voltage ratio, discharge-to-total voltage ratio, grid separation ratio, and accelerator hole diameter ratio. The ion extraction performance generally increases with increased ratios of the accelerator hole diameter ratio; however, when operating in the range of medium-to-high ratios of net-to-total accelerating voltage at small grid separation ratios, the highest beam current densities are observed at accelerator-to-screen grid hole diameter ratios less than unity. Levels of high beam current per hole are realized for a specified net accelerating voltage at low net-to-total accelerating voltage levels for all grid separation ratios. At small grid separation ratios, there is another high beam current per hole operating point that is realized at an optimum net-to-total accelerating voltage ratio in the range $R = 0.5$-0.8.

The electron backstreaming data obtained in this study resulted in a simple design curve that can be used to predict electron backstreaming in two-grid accelerator systems.

Acknowledgment

This work was performed under NASA Grant NGR-06-002-112.

References

[1]Lockwood, D. L., Michelson, W., and Hamza, V., "Analytical Space-Charge Flow and Theoretical Electrostatic Rocket Engine Performance," Paper presented at 1st Electric Propulsion Conference, Berkeley, Calif., March 1962.

[2]Hyman, J., Eckhardt, W. O., Knechtli, R. C., and Buckey, C. R., "Formation of Ion Beams from Plasma Sources: Part 1," *AIAA Journal,* Vol. 2, Oct. 1964, pp. 1739-1748.

[3]Bogart, C. D. and Richley, E. A., "A Space Charge Flow Computer Program," NASA TN-D3394, 1966.

[4]Lathem, W. C., "Ion Accelerator Designs for Kaufman Thrusters," *Journal of Spacecraft and Rockets,* Vol. 6, Nov. 1969, p. 1237.

[5]Kaufman, H. R., "Accelerator System Solution for Broad-Beam Ion Sources," *AIAA Journal,* Vol. 15, July 1977, pp. 1025-1034.

[6]Alterburg, W., Freisinger, J., Hauser, J. Seibert, N., and Loeb, H. W., "Beam Formation in RF-Ion Thrusters," AIAA Paper 75-426, 1975.

[7]Aston, G. and Kaufman, H. R., "The Ion-Optics of a Two-Grid Electron Bombardment Thruster," AIAA Paper 76-1029, 1976.

[8]Aston, G., Kaufman, H. R., and Wilbur, P. J., "Ion Beam Divergence Characteristics of Two-Grid Accelerator Systems," *AIAA Journal,* Vol. 16, May 1978, pp. 516-524.

[9]Aston, G. and Kaufman, H. R., "Ion Beam Divergence Characteristics of Three-Grid Accelerator Systems," *AIAA Journal,* Vol. 17, Jan. 1979, pp. 64-70.

[10]Homa, J. H. and Wilbur, P. J., "Ion Beamlet Vectoring by Grid Translation," AIAA Paper 82-1895, Nov. 1982.

[11]Kaufman, H. R., "Ion Source Design for Industrial Applications," *AIAA Journal,* Vol. 20, June 1982, pp. 745-760.

[12]Aston, G. and Wilbur, P. J., "Ion Extraction from a Plasma," *Journal of Applied Physics,* Vol. 52, April 1981, pp. 2614-2626.

[13]Rovang, D. C., "Ion Extraction Capabilities of Two-Grid Accelerator Systems," NASA CR-174621, Feb. 1984.

[14]Brophy, J. R., "Effect of Screen Grid Potential on Perveance," appears in "Advanced Ion Thruster Research," NASA CR-168340, Jan. 1984.

[15]Rovang, D. C. and Wilbur, P. J., "Ion Extraction Capabilities of Very Closely Spaced Grids," AIAA Paper 82-1895, Nov. 1982.

[16]Tsuchiya, I. and Masuzawa, T., "Study on Low Energy Ion-milling Equipment," *Proceedings of International Ion Engineering Congress, Institute of Electrical Engineers of Japan,* Kyoto, Japan, Sept. 1983, pp. 765-770.

[17]Hudson, Wayne, "Auxiliary Propulsion Thruster Performance with Ion Machined Accelerator Grids," AIAA Paper 75-4215, March 1975.

[18]Kerslake, W. R. and Pawlik, E. V., "Additional Studies of Screen and Accelerator Grids for Electron-Bombardment Ion Thrusters," NASA TN D-1411, 1963.

[19]Rawlin, V. K., Banks, B. A., and Byers, D. C., "Dished Accelerator Grids on 30-cm Ion Thruster," *Journal of Spacecraft and Rockets,* Vol. 10, Jan. 1973, pp. 29-35.

[20]Rawlin, V. K., "Studies of Dished Accelerator Grids for 30-cm Ion Thrusters," AIAA Paper 73-1086, Oct./Nov. 1973.

[21]Kaufman, H. R., "Technology of Electron Bombardment Thrusters," *Advances in Electronics and Physics,* Vol. 36, Academic Press, San Francisco, 1974.